Title

Transcranial chronic optical access to longitudinally measure cerebral blood flow

Authors

Hoover, Evelyn M

Crouzet, Christian

Bordas, Julianna M

et al.

Publication Date

2021-02-01

DOI

10.1016/j.jneumeth.2020.109044

Peer reviewed

HHS Public Access

Author manuscript

J Neurosci Methods. Author manuscript; available in PMC 2022 February 15.

Published in final edited form as:

J Neurosci Methods. 2021 February 15; 350: 109044. doi:10.1016/j.jneumeth.2020.109044.

Transcranial chronic optical access to longitudinally measure cerebral blood flow

Evelyn M. Hoover[a,b], **Christian Crouzet**[c,d], **Julianna M. Bordas**[c,d], **Dario X. Figueroa Velez**[e,f], **Sunil P. Gandhi**[e,f], **Bernard Choi**[c,d,g,h], **Melissa B. Lodoen**[a,b,*]

[a]University of California Irvine, Department of Molecular Biology and Biochemistry, Irvine, USA, 92697

[b]University of California Irvine, Institute for Immunology, Irvine, USA, 92697

[c]University of California Irvine, Department of Biomedical Engineering, Irvine, USA, 92697

[d]University of California Irvine, Beckman Laser Institute and Medical Clinic, Irvine, USA, 92697

[e]University of California Irvine, Department of Neurobiology and Behavior, Irvine, USA, 92697

[f]University of California Irvine, Center for the Neurobiology of Learning and Memory, Irvine, USA, 92697

[g]University of California Irvine, Department of Surgery, Irvine, USA, 92697

[h]University of California Irvine, Edwards Lifesciences Center for Advanced Cardiovascular Technology, Irvine, USA

Abstract

Background: Regulation of cerebral blood flow is critical for normal brain functioning, and many physiological and pathological conditions can have long-term impacts on cerebral blood flow. However, minimally invasive tools to study chronic changes in animal models are limited.

New Method: We developed a minimally invasive surgical technique (Cyanoacrylate skull, CAS) allowing us to image cerebral blood flow longitudinally through the intact mouse skull using laser speckle imaging.

[*]Melissa B. Lodoen, mlodoen@uci.edu.

CRediT authorship contribution statement

Evelyn Hoover: Conceptualization, Methodology, Formal analysis, Investigation, Writing - Original Draft, Writing - Review & Editing. **Christian Crouzet:** Methodology, Software, Formal analysis, Investigation, Writing - Review & Editing. **Julianna M. Bordas:** Methodology, Investigation, Writing - Review & Editing. **Dario X. Figueroa Velez:** Methodology, Writing - Review & Editing. **Sunil P. Gandhi:** Methodology, Resources, Writing - Review & Editing. **Bernard Choi:** Methodology, Resources, Writing - Review & Editing, Supervision. **Melissa B. Lodoen:** Conceptualization, Methodology, Resources, Writing - Review & Editing, Supervision.

Declaration of Competing Interest

None.

Results: With CAS we were able to detect acute changes in cerebral blood flow induced by hypercapnic challenge. We were also able to image cerebral blood flow dynamics with laser speckle imaging for over 100 days. Furthermore, the relative cerebral blood flow remained stable in mice from 30 days to greater than 100 days after the surgery.

Comparison with Existing Methods: Previously, achieving continuous long-term optical access to measure cerebral blood flow in individual vessels in a mouse model involved invasive surgery. In contrast, the CAS technique presented here is relatively non-invasive, as it allows stable optical access through an intact mouse skull.

Conclusions: The CAS technique allows researcher to chronically measure cerebral blood flow dynamics for a significant portion of a mouse's lifespan. This approach may be useful for studying changes in blood flow due to cerebral pathology or for examining the therapeutic effects of modifying cerebral blood flow in mouse models relevant to human disease.

Keywords

cerebral blood flow; circulation; laser speckle imaging; in vivo imaging; brain; surgery

1 Introduction

Cerebral blood flow (CBF) regulation is essential for normal brain functioning, and many physiological and pathological conditions may cause disruption in CBF. Stroke (Siegel et al., 2015), Alzheimer's disease (Kogure et al., 2000; Ruitenberg et al., 2005), and aging (Martin et al., 1991) can have long-lasting negative effects on CBF, whereas acute infection, such as with SARS-CoV2, can cause short-term effects on CBF in Covid-19 patients (Helms et al., 2020; Soldatelli et al., 2020). There are currently few techniques to study long-term CBF changes or the efficacy of therapeutic modulation of CBF in animal models.

The ability to measure CBF in the same animals longitudinally over time has several advantages. First, it reduces the number of experimental animals needed to examine the kinetics of CBF changes, as researchers can investigate CBF dynamics in the same set of mice, rather than euthanizing separate cohorts of mice for each time-point. Second, the ability to determine a baseline measurement of CBF before a pathology manifests or prior to induced changes in blood flow controls for inter-animal variation in CBF, as each animal can serve as its own internal control. Current approaches for measuring CBF in animal models include methods based on magnetic resonance imaging (Calamante et al., 1999), positron emission tomography (Heiss et al., 1994), microscopy, such as two-photon excitation fluorescence microscopy (Drew et al., 2010; Kleinfeld et al., 1998; Schaffer et al., 2006; Shih et al., 2015; Zhang and Murphy, 2007), and wide-field optical techniques like laser speckle imaging (LSI) (Boas and Dunn, 2010; Dunn et al., 2001; Fercher and Briers, 1981). Among these techniques, only two-photon microscopy and LSI provide the spatial resolution necessary to image individual blood vessels (Dunn et al., 2001; Shih et al., 2012).

LSI has been used to measure CBF dynamics in a wide-range of neurologically relevant conditions, such as cardiac arrest (Crouzet et al., 2016), cortical spreading depression (Dunn et al., 2001), and stroke (Schrandt et al., 2015; Sunil et al., 2020). Unlike two-photon

microscopy, which enables absolute measurements of cerebral blood flow, LSI detects relative blood flow in biological tissues (Boas and Dunn, 2010; Dunn et al., 2001; Fercher and Briers, 1981). However, LSI involves a simpler imaging platform and does not require the use of exogenous dyes or transgenic animals with fluorescently labeled vasculature (e.g. Tie2-GFP mice) to visualize the dynamics of flow in cerebral vessels (Drew et al., 2010; Kleinfeld et al., 1998; Schaffer et al., 2006; Shih et al., 2015; Zhang and Murphy, 2007).

An important consideration in imaging cerebral blood flow is balancing clear optical access with the potential for damage inflicted by a surgical procedure. Craniotomy and skull-thinning surgeries can provide optimal access for two-photon microscopy and LSI. However, these approaches require highly precise surgical skill to avoid inducing permeability of the blood-brain barrier (BBB) due to heat from drilling (Luan et al., 2017; Shoffstall et al., 2018). Removing a portion of the skull may also cause a temporary inflammatory response or induce bone re-growth, resulting in diminished optical access (Xu et al., 2007). LSI does not require a craniotomy or skull-thinning surgery, since this technique can be done through the intact hydrated skull of mice once the scalp is resected (Ayata et al., 2004b). Resecting the scalp is a simpler surgical procedure than craniotomy or skull thinning. The shorter time-frame for surgery may increase the number of animals a researcher can reasonably include in a study (since a craniotomy can require 4 or more hours to perform (Goldey et al., 2014)), while also reducing the length of time that each animal is under anesthesia. However, to our knowledge, there have been no reports of maintaining long-term optical access to measure CBF with LSI through an intact skull.

Here we describe a surgical method in mice that we have named cyanoacrylate skull (CAS), which enables continuous chronic optical access through an intact skull. The CAS approach enables bi-hemispheric imaging of cerebral blood vessels using LSI or other wide-field optical imaging techniques. Using CAS, we were able to stably measure functional CBF for more than 100 days post-surgery and detect acute changes in CBF due to hypercapnia (elevated CO_2). This procedure can take a skilled researcher less than one hour to complete, which is significantly less time than performing a craniotomy. The CAS technique may prove useful for researchers investigating relative cerebral blood flow, as it will enable studies on changes in long-term CBF in human-relevant disease models (e.g. Alzheimer's disease, stroke, infection), as well as the ability to evaluate therapy-induced CBF changes over time.

2 Materials and Methods

2.1 Animals

All procedures and protocols were approved by the Institutional Animal Care and Use Committee at the University of California, Irvine. Procedures were performed on 2–5 month-old male and female C57BL/6J mice purchased from Jackson Laboratories.

2.2 Surgical Preparation

A schematic of the surgery is shown in Fig. 1A, and accompanying images of each step of the surgery are shown in Fig. 1B–E. Mice were anesthetized with O_2 vaporized isoflurane

(2% for induction, 1–1.5% for maintenance, Patterson Veterinary, Devens, MA). Body temperature was maintained at 37°C with a feedback heating pad (Harvard Apparatus, Holliston, MA). Sterile eye ointment (Rugby, Livonia, MI) was applied to prevent corneal drying. Carprofen (10 mg/kg, s.c., Zoetis) and topical 2% lidocaine hydrochloride jelly (Akorn, Lake Forest, IL) were administered to provide systemic and local analgesia, respectively. Mice were given Ringer's lactate solution (0.2 mL/20 g/hr, s.c.) to replace fluids. All surgical tools were sterilized using a glass bead sterilizer (Germinator 500). Following shaving and sterilization with Povidone-iodine for five minutes, the scalp was resected to expose bregma and lambda. 2% lidocaine hydrochloride jelly was reapplied to the exposed fascia (Fig. 1B, Supplemental Video 1), which was subsequently removed. Afterwards, the skull was dried with ethanol (70% in DI water) (Fig. 1C, Supplemental Video 1). Three thin layers of cyanoacrylate (Vetbond, 3M) were applied using a double-ended micro spatula (Fine Science Tools). Each layer was composed of a single drop of cyanoacrylate (~15 μL) and allowed to dry between applications to ensure smoothness (Fig. 1D, Supplemental Video 1). Multiple layers of cyanoacrylate prevented potential skull exposure from the mice, as they occasionally scratch at the surface. After the cyanoacrylate layers were dry, a ~2 mm deep well was then made using acrylic resin Ortho-Jet BCA (Lang Dental, Wheeling, IL) around the edges of the surgical prep, and a final thin layer of cyanoacrylate was applied over the previous cyanoacrylate layers (Fig. 1E, Supplemental Video 1). A second dose of Carprofen (10 mg/kg, s.c., Zoetis) was administered one day post-operation (dpo). Mice were not returned to their home cages until their skulls were uniformly covered with cyanoacrylate to prevent infection. After the procedure, mice can be co-housed and handled as normal (i.e., being held by the scruff for injections). No signs of distress (i.e. low activity, hunched poster, or piloerection) were noted. Animals were allowed to recover from the surgery for 3–5 days before longitudinal imaging was performed.

2.3 Imaging Instrumentation

To obtain cerebral blood flow (CBF) data, we used laser speckle imaging (LSI) (Crouzet et al., 2016; Dunn et al., 2001). A schematic of the setup is shown in Fig. 2A. A long-coherence 785 nm laser (Ondax, Monrovia, CA) was used as the excitation source. Laser light was transmitted through beam expansion optics, which included an aspheric lens (ThorLabs, Newton, NJ) and ground glass diffuser (ThorLabs, Newton, NJ), to achieve near-uniform illumination of the cortex. Raw speckle images (10 ms exposure time) were acquired using a 4x Achrovid objective with a 37 mm working distance (Edmund Optics, Barrington, NJ) and monochrome CMOS camera (FLIR, Wilsonville, OR). Cross-polarization optics between the source and detector were used to remove specular reflection.

2.4 Imaging, Data Acquisition, and Data Processing

For imaging, mice were anesthetized with O_2 vaporized isoflurane (2% for induction and 1.5% for maintenance, Patterson Veterinary, Devens, MA). Sterile eye ointment (Rugby, Livonia, MI) was applied to prevent corneal drying. Body temperature was maintained at 37° C with a feedback heating pad (Harvard Apparatus, Holliston, MA), as described above. Saline was then applied to the cyanoacrylate and a glass coverslip (Fisherbrand, 12CIR-2) was placed on top for 10 min prior to image acquisition to allow the relative blood flow to

stabilize. Total imaging time takes approximately 14 minutes per mouse. Each mouse was imaged 11 to 14 times over 105 days.

Raw speckle images were acquired at 60 Hz using a LabVIEW (National Instruments, Austin, TX) program. First, all raw speckle images were converted to CBF maps using the spatial speckle contrast algorithm to detect periods of motion artifact. A 5 x 5 sliding window was used to convert each raw speckle image to a corresponding speckle contrast (K) image using the equation $K = \sigma/< I >$, where σ is the standard deviation of the intensity and <I> is the average intensity within each sliding window position. Each speckle contrast image was then converted to a CBF map using a simplified speckle imaging equation $CBF = \frac{1}{2TK^2}$ (Ramirez-San-Juan et al., 2008). Next, sharp spikes due to breathing were manually defined in the CBF time course as periods of motion artifact. These time points were removed from the calculation of the temporal speckle contrast.

MATLAB (MathWorks, Natick, MA) code was written to convert raw speckle images to CBF maps using the temporal speckle contrast algorithm (Cheng et al., 2003). The temporal algorithm was chosen, as it is less susceptible to static scatterers, such as the skull, than the spatial algorithm (Li et al., 2006; Ramirez-San-Juan et al., 2014). Speckle contrast (K) was calculated as the ratio between the standard deviation and the mean intensity at each pixel over 60 raw speckle images without motion artifact caused by breathing. A 3x3 spatial averaging filter was then applied to the temporal speckle contrast image to reduce noise. Each speckle contrast image was then converted to a CBF map using a simplified speckle imaging equation $CBF = \frac{1}{2TK^2}$, where T is the exposure time (Ramirez-San-Juan et al., 2014).

2.5 Hypercapnia Experiments

Mice were imaged continuously for 15 minutes. For the first 5 minutes, they breathed room air to establish baseline readings. Then they were challenged for 5 min with 5% CO_2 with balanced room air to induce hypercapnia, and for the last 5 minutes they breathed room air (Fig. 3A).

2.6 Data Quantification

To assess longitudinal CBF changes using the CAS preparation, speckle contrast images at each time point were aligned using MATLAB code (Lertsakdadet et al., 2018). Using the aligned data, a point at bregma and lambda were selected. Two semi-elliptical regions of interest (ROIs) offset by +/− 0.5 mm from the midline with radii of 1.05 mm along the short axis and 1.63 mm along the long axis. were used to obtain longitudinal CBF data. The same ROI per animal was used for every time point. A representative example of ROI selection is shown in Fig. 2B–D. The median CBF from each ROI was calculated, and the median CBF values for the right and left hemispheres were averaged and used for further statistical analyses. In the case of one mouse (Fig 2E, light blue), only the CBF from the right hemisphere was included, as the other ROI had a scattering artifact due to an uneven coating of cyanoacrylate or to insufficient removal of fascia.

To assess hypercapnia-induced CBF changes, the spatial speckle contrast algorithm was used. For each imaged mouse, four ROIs were selected. The two semi-elliptical ROIs (described above) were used to obtain a more global CBF measurement. Two small ROIs (one left hemisphere, one right hemisphere) were also defined. A representative example of the ROI selection is shown in Fig. 3B. For each ROI, a CBF time course was obtained. A 10s sliding median filter was applied to the CBF time courses to remove the pulsatile component. The median-filtered data was downsampled to a sampling frequency of 1Hz. The downsampled data was then normalized to the mean median-filtered CBF calculated over a one-minute interval immediately prior to onset of hypercapnia to create a rCBF time course.

In addition, we determined the smallest vessels that could be resolved in this system by analyzing images from a subset of the mice in ImageJ. First, we applied an automated threshold to detect vessels, created a mask, and smoothed the resulting image with a Guassian blur (sigma set to 0.75). With this procedure, vessels as small as 40 μm could be resolved.

2.6 Statistical Analysis

GraphPad Prism 7.02 software was used for statistical analyses. A two-way repeated measures ANOVA followed by a post-hoc Tukey test was used to test the left and right hemispheres, as well as the small and large ROIs for significant differences in rCBF after the start of the hypercapnia challenge from baseline (average of 5 minutes prior to hypercapnia). Differences between groups in the longitudinal imaging dataset were determined using a repeated measures one-way ANOVA, followed by a post-hoc Tukey test. $P < 0.05$ was considered significant.

3 Results & Discussion

We used LSI to measure the CBF of seven mice (four females and three males) for the first two weeks after implementation of the CAS surgical technique (Fig. 2E). CBF values from the right and left hemisphere were averaged to account for the blood flow changes across both hemispheres (Fig. 2D and E).

To assess our ability to detect dynamic CBF changes using LSI after the CAS technique, a hypercapnia challenge induced by CO_2 inhalation was performed (Fig. 3A). Hypercapnia is commonly used as a way to assess cerebrovascular reactivity, as it causes a rapid increase in CBF (Ayata et al., 2004a; Dalkara et al., 1995; A Hauge et al., 1980; Wenzel et al., 2020). Consistent with prior studies (Ayata et al., 2004a; Dalkara et al., 1995; Anton Hauge et al., 1980; Wenzel et al., 2020), we detected a significant increase in rCBF in both the left hemisphere (Fig. 3C) and the right hemisphere (Fig. 3D). These data indicate that acute changes in CBF can be detected by LSI imaging of mice that have undergone the CAS surgical technique. Both large and small ROIs were examined for comparison, and no statistically significant differences between the large and small ROIs, nor the left and right hemispheres were detected. These data indicate that the size of the ROI drawn did not affect the measurement of relative changes in the CBF.

To determine the length of time over which we could maintain optical access for LSI imaging using the CAS technique, we continued to image a subset of mice (two females and two males) for more than 100 dpo. Representative speckle contrast images are shown for 5, 37, 54, and 105 dpo (Fig. 4A), and CBF values are shown for all time points (Fig. 4B). Over time, there appeared to be a decline in CBF in the mice. To examine this trend, we grouped the animals into three categories: early (<1 month-post-surgery), middle (1–2 month(s)-post-surgery), and late (2+ months-post-surgery) (Fig. 4C). In aggregating the data in this manner, CBF was found to be significantly higher in the early phase post-surgery when compared to the middle and late phases, with no difference between the middle and late phases. Therefore, these data suggest that the surgical procedure may induce a temporary increase in CBF, or that the CBF values decline after the early phase and then stabilize with time after surgery.

4 Conclusions

As emerging research reveals that many physiological and pathological conditions affect CBF, reproducible and minimally invasive tools are needed to study changes in CBF in animal models. Though CAS may not have the resolution of techniques that rely on craniotomies for optical access, it has numerous benefits for detecting CBF using LSI. The surgery is relatively fast, easy to master, and less invasive than techniques that involve removing the skull. As we have demonstrated, CAS can be used prior to LSI for detecting acute changes in rCBF (as shown by hypercapnic challenge), as well as for imaging experiments in mice that last over 100 days.

Notably, our data indicate that CBF measurements stabilized after the initial two weeks post-operation. Based on these findings, it may be recommended to begin “baseline” imaging after this point. Another consideration is the use of anesthesia for imaging. In the current study, mice were imaged with isoflurane anesthesia, which has been previously shown to increase CBF (Janssen et al., 2004). In the future, this technique may be refined to allow for imaging of head-constrained awake mice, similar to the method published by Murphy *et al.* (Murphy et al., 2016).

We anticipate that CAS will be a useful surgical preparation for investigating diseases that affect CBF, including processes that take several months to develop (such as models of Alzheimer’s disease), as it enables the study of long-term changes in CBF. CAS coupled with LSI imaging may also be useful for analyzing the potential benefits of therapeutics administered to alter CBF. This approach should mitigate any potential effects of ananesthetic agent on CBF measurements. Ultimately, CAS may enhance the understanding and discovery of therapeutics for diseases that result in altered CBF in humans.

Supplementary Material

Refer to Web version on PubMed Central for supplementary material.

Acknowledgments

We thank all members of the Lodoen, Choi, Gandhi, Morrissette, and Andrade labs for their helpful discussions on this project. This work was supported by National Institutes of Health R01 AI120846 (to M.B.L), American Cancer Society 126688-RSG-14-202-01-MPC (to M.B.L.), National Institutes of Health R21 AG066000 (to B.C.), National Institutes of Health R01 1R01EY029490-01A1 (to S.P.G.), National Institutes of Health T32AI060573 (to E.M.H.), National Institutes of Health T32GM008620 (to E.M.H.), National Institutes of Health 5TL1TR001415-06 (to C.C.), American Heart Association Predoctoral Fellowship 19PRE34380476 (to E.M.H.), as well as the Arnold and Mabel Beckman Foundation.

References

Ayata C, Dunn AK, Gursoy-Özdemir Y, Huang Z, Boas DA, Moskowitz MA, 2004a. Laser speckle flowmetry for the study of cerebrovascular physiology in normal and ischemic mouse cortex. J. Cereb. Blood Flow Metab. 24, 744–755. 10.1097/01.WCB.0000122745.72175.D5 [PubMed: 15241182]

Ayata C, Shin HK, Salomone S, Ozdemir-Gursoy Y, Boas DA, Dunn AK, Moskowitz MA, 2004b. Pronounced Hypoperfusion during Spreading Depression in Mouse Cortex. J. Cereb. Blood Flow Metab. 24, 1172–1182. 10.1097/01.WCB.0000137057.92786.F3 [PubMed: 15529018]

Boas DA, Dunn AK, 2010. Laser speckle contrast imaging in biomedical optics. J. Biomed. Opt. 15, 11109. 10.1117/1.3285504

Calamante F, Thomas DL, Pell GS, Wiersma J, Turner R, 1999. Measuring Cerebral Blood Flow Using Magnetic Resonance Imaging Techniques. J. Cereb. Blood Flow Metab. 19, 701–735. 10.1097/00004647-199907000-00001Pre-proof [PubMed: 10413026]

Cheng H, Luo Q, Zeng S, Chen S, Cen J, Gong H, 2003. Modified laser speckle imaging method with improved spatial resolution. J. Biomed. Opt. 8, 559. 10.1117/1.1578089 [PubMed: 12880364]

Crouzet C, Wilson RH, Bazrafkan A, Farahabadi MH, Lee D, Alcocer J, Tromberg BJ, Choi B, Akbari Y, 2016. Cerebral blood flow is decoupled from blood pressure and linked to EEG bursting after resuscitation from cardiac arrest. Biomed. Opt. Express 7, 4660–4673. 10.1364/BOE.7.004660 [PubMed: 27896005]

Dalkara T, Irikura K, Huang Z, Panahian N, Moskowitz MA, 1995. Cerebrovascular responses under controlled and monitored physiological conditions in the anesthetized mouse. J. Cereb. blood flow Metab. Off. J. Int. Soc. Cereb. Blood Flow Metab 15, 631–638. 10.1038/jcbfm.1995.78

Drew PJ, Shih AY, Driscoll JD, Knutsen PM, Blinder P, Davalos D, Akassoglou K, Tsai PS, Kleinfeld D, 2010. Chronic optical access through a polished and reinforced thinned skull. Nat. Methods 7, 981–984. 10.1038/nmeth.1530 [PubMed: 20966916]

Dunn AK, Bolay H, Moskowitz MA, Boas DA, 2001. Dynamic Imaging of Cerebral Blood Flow Using Laser Speckle. J. Cereb. Blood Flow Metab. 21, 195–201. 10.1097/00004647-200103000-00002 [PubMed: 11295873]

Fercher AF, Briers JD, 1981. Flow visualization by means of single-exposure speckle photography. Opt. Commun. 37, 326–330. 10.1016/0030-4018(81)90428-4

Goldey GJ, Roumis DK, Glickfeld LL, Kerlin AM, Reid RC, Bonin V, Schafer DP, Andermann ML, 2014. Removable cranial windows for long-term imaging in awake mice. Nat. Protoc. 9, 2515–2538. 10.1038/nprot.2014.165 [PubMed: 25275789]

Hauge A, Thoresen M, Walløe L, 1980. Changes in cerebral blood flow during hyperventilation and CO2-breathing measured transcutaneously in humans by a bidirectional, pulsed, ultrasound Doppler blood velocitymeter. Acta Physiol. Scand. 110, 167–173. 10.1111/j.1748-1716.1980.tb06647.x [PubMed: 6782831]

Hauge, Anton, Thoresen M, Walløe L, 1980. Changes in cerebral blood flow during hyperventilation and CO2- breathing measured transcutaneously in humans by a bidirectional, pulsed, ultrasound doppler blood velocitymeter. Acta Physiol. Scand. 110, 167–173. 10.1111/j.1748-1716.1980.tb06647.x [PubMed: 6782831]

Heiss WD, Graf R, Wienhard K, Löttgen J, Saito R, Fujita T, Rosner G, Wagner R, 1994. Dynamic Penumbra Demonstrated by Sequential Multitracer PET after Middle Cerebral Artery Occlusion in Cats. J. Cereb. Blood Flow Metab. 14, 892–902. 10.1038/jcbfm.1994.120 [PubMed: 7929654]

Helms J, Kremer S, Merdji H, Clere-Jehl R, Schenck M, Kummerlen C, Collange O, Boulay C, Fafi-Kremer S, Ohana M, Anheim M, Meziani F, 2020. Neurologic Features in Severe SARS-CoV-2 Infection. N. Engl. J. Med. 382, 2268–2270. 10.1056/NEJMc2008597 [PubMed: 32294339]

Janssen BJA, De Celle T, Debets JJM, Brouns AE, Callahan MF, Smith TL, 2004. Effects of anesthetics on systemic hemodynamics in mice. Am. J. Physiol. Circ. Physiol 287, H1618–H1624. 10.1152/ajpheart.01192.2003

Kleinfeld D, Mitra PP, Helmchen F, Denk W, 1998. Fluctuations and stimulus-induced changes in blood flow observed in individual capillaries in layers 2 through 4 of rat neocortex. Proc. Natl. Acad. Sci. 95, 15741 LP–15746. 10.1073/pnas.95.26.15741 [PubMed: 9861040]

Kogure D, Matsuda H, Ohnishi T, Asada T, Uno M, Kunihiro T, Nakano S, Takasaki M, 2000. Longitudinal evaluation of early Alzheimer's disease using brain perfusion SPECT. J. Nucl. Med. 41, 1155–1162. [PubMed: 10914904]

Lertsakdadet B, Yang BY, Dunn CE, Ponticorvo A, Crouzet C, Bernal N, Durkin AJ, Choi B, 2018. Correcting for motion artifact in handheld laser speckle images. J. Biomed. Opt. 23, 1–7. 10.1117/1.JBO.23.3.036006

Li P, Ni S, Zhang L, Zeng S, Luo Q, 2006. Imaging cerebral blood flow through the intact rat skull with temporal laser speckle imaging. Opt. Lett. 31, 1824–1826. 10.1364/OL.31.001824 [PubMed: 16729083]

Luan L, Wei X, Zhao Z, Siegel JJ, Potnis O, Tuppen CA, Lin S, Kazmi S, Fowler RA, Holloway S, Dunn AK, Chitwood RA, Xie C, 2017. Ultraflexible nanoelectronic probes form reliable, glial scar–free neural integration. Sci. Adv. 3, e1601966. 10.1126/sciadv.1601966 [PubMed: 28246640]

Martin AJ, Friston KJ, Colebatch JG, Frackowiak RSJ, 1991. Decreases in Regional Cerebral Blood Flow with Normal Aging. J. Cereb. Blood Flow Metab. 11, 684–689. 10.1038/jcbfm.1991.121 [PubMed: 2050757]

Murphy TH, Boyd JD, Bolaños F, Vanni MP, Silasi G, Haupt D, Ledue JM, 2016. High-throughput automated home-cage mesoscopic functional imaging of mouse cortex. Nat. Commun. 7, 11611. 10.1038/ncomms11611 [PubMed: 27291514]

Ramirez-San-Juan JC, Ramos-Garcia R, Guizar-Iturbide I, Martinez-Niconoff G, Choi B, 2008. Impact of velocity distribution assumption on simplified laser speckle imaging equation. Opt. Express 16, 3197–3203. 10.1364/OE.16.003197 [PubMed: 18542407]

Ramirez-San-Juan JC, Regan C, Coyotl-Ocelotl B, Choi B, 2014. Spatial versus temporal laser speckle contrast analyses in the presence of static optical scatterers. J. Biomed. Opt. 19, 106009. 10.1117/1.JBO.19.10.106009 [PubMed: 25334006]

Ruitenberg A, den Heijer T, Bakker SLM, van Swieten JC, Koudstaal PJ, Hofman A, Breteler MMB, 2005. Cerebral hypoperfusion and clinical onset of dementia: The Rotterdam study. Ann. Neurol. 57, 789–794. 10.1002/ana.20493 [PubMed: 15929050]

Schaffer CB, Friedman B, Nishimura N, Schroeder LF, Tsai PS, Ebner FF, Lyden PD, Kleinfeld D, 2006. Two-photon imaging of cortical surface microvessels reveals a robust redistribution in blood flow after vascular occlusion. PLoS Biol. 4, 258–270. 10.1371/journal.pbio.0040022

Schrandt CJ, Kazmi SMS, Jones TA, Dunn AK, 2015. Chronic Monitoring of Vascular Progression after Ischemic Stroke Using Multiexposure Speckle Imaging and Two-Photon Fluorescence Microscopy. J. Cereb. Blood Flow Metab. 35, 933–942. 10.1038/jcbfm.2015.26 [PubMed: 25712498]

Shih AY, Driscoll JD, Drew PJ, Nishimura N, Schaffer CB, Kleinfeld D, 2012. Two-Photon Microscopy as a Tool to Study Blood Flow and Neurovascular Coupling in the Rodent Brain. J. Cereb. Blood Flow Metab. 32, 1277–1309. 10.1038/jcbfm.2011.196 [PubMed: 22293983]

Shih AY, Rühlmann C, Blinder P, Devor A, Drew PJ, Friedman B, Knutsen PM, Lyden PD, Matéo C, Mellander L, Nishimura N, Schaffer CB, Tsai PS, Kleinfeld D, 2015. Robust and fragile aspects of cortical blood flow in relation to the underlying angioarchitecture. Microcirculation 22, 204–218. 10.1111/micc.12195 [PubMed: 25705966]

Shoffstall AJ, Paiz JE, Miller DM, Rial GM, Willis MT, Menendez DM, Hostler SR, Capadona JR, 2018. Potential for thermal damage to the blood–brain barrier during craniotomy: implications for intracortical recording microelectrodes. J. Neural Eng. 15, 34001. 10.1088/1741-2552/aa9f32

Siegel JS, Snyder AZ, Ramsey L, Shulman GL, Corbetta M, 2015. The effects of hemodynamic lag on functional connectivity and behavior after stroke. J. Cereb. Blood Flow Metab. 36, 2162–2176. 10.1177/0271678X15614846 [PubMed: 26661223]

Soldatelli MD, Amaral L.F. do, Veiga VC, Rojas SSO, Omar S, Marussi VHR, 2020. Neurovascular and perfusion imaging findings in coronavirus disease 2019: Case report and literature review. Neuroradiol. J. 33, 368–373. 10.1177/1971400920941652 [PubMed: 32666873]

Sunil S, Erdener SE, Lee BS, Postnov D, Tang J, Kura S, Cheng X, Chen DIAA, Kiliç K, 2020. Awake chronic mouse model of targeted pial vessel occlusion via photothrombosis. Neurophotonics 7, 1. 10.1117/1.nph.7.1.015005

Wenzel J, Hansen CE, Bettoni C, Vogt MA, Lembrich B, Natsagdorj R, Huber G, Brands J, Schmidt K, Assmann JC, Stölting I, Saar K, Sedlacik J, Fiehler J, Ludewig P, Wegmann M, Feller N, Richter M, Müller-Fielitz H, Walther T, König GM, Kostenis E, Raasch W, Hübner N, Gass P, Offermanns S, De Wit C, Wagner CA, Schwaninger M, 2020. Impaired endothelium-mediated cerebrovascular reactivity promotes anxiety and respiration disorders in mice. Proc. Natl. Acad. Sci. U. S. A. 117, 1753–1761. 10.1073/pnas.1907467117 [PubMed: 31896584]

Xu H-T, Pan F, Yang G, Gan W-B, 2007. Choice of cranial window type for in vivo imaging affects dendritic spine turnover in the cortex. Nat. Neurosci. 10, 549–551. 10.1038/nn1883 [PubMed: 17417634]

Zhang S, Murphy TH, 2007. Imaging the impact of cortical microcirculation on synaptic structure and sensory-evoked hemodynamic responses in vivo. PLoS Biol. 5, 1152–1167. 10.1371/journal.pbio.0050119

Highlights

- Many pathological conditions can cause long-term negative effects on cerebral blood flow.
- Laser speckle imaging enables minimally invasive measurement of cerebral blood flow in the mouse.
- We developed a surgical technique that permits continuous and chronic optical access through the intact mouse skull.
- This approach enables longitudinal bi-hemispheric imaging of cerebral blood vessels.
- We measured cerebral blood flow through the mouse skull longitudinally for over 100 days.

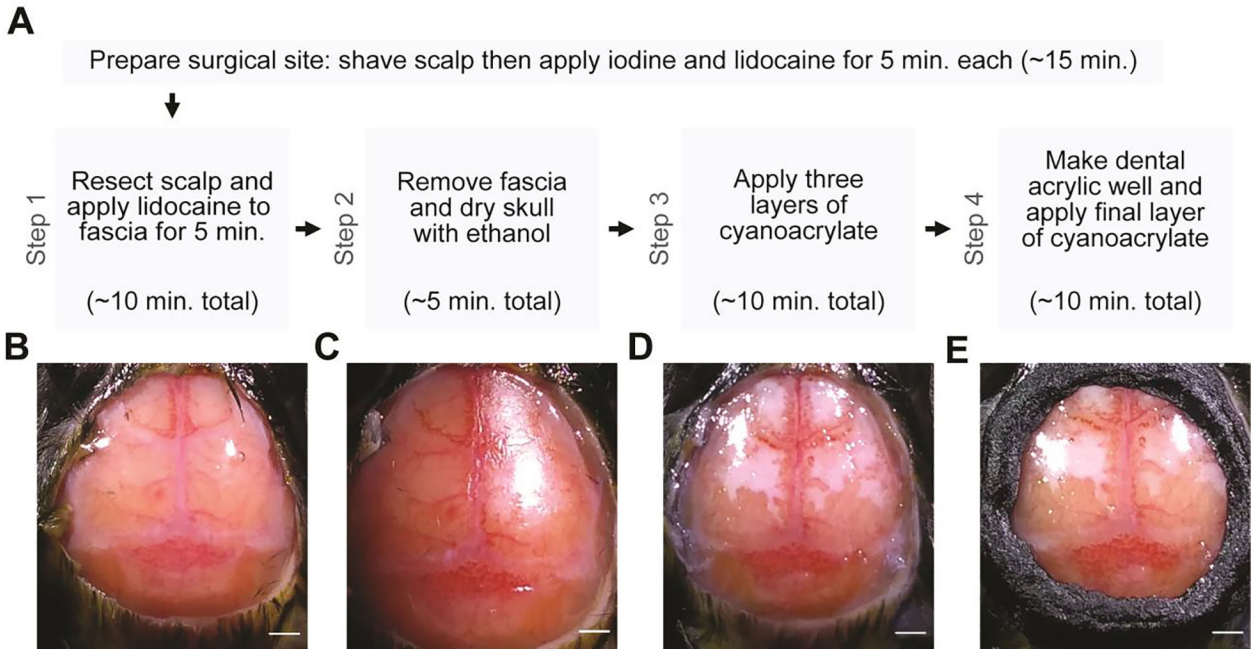

Fig. 1. Surgical procedure for chronic optical access.

A) Flowchart showing steps for the surgical procedure, as well as the approximate time that it takes to complete each step. B-E) Representative image of surgical site after each step of the surgical procedure. Scale bars: 1 mm.

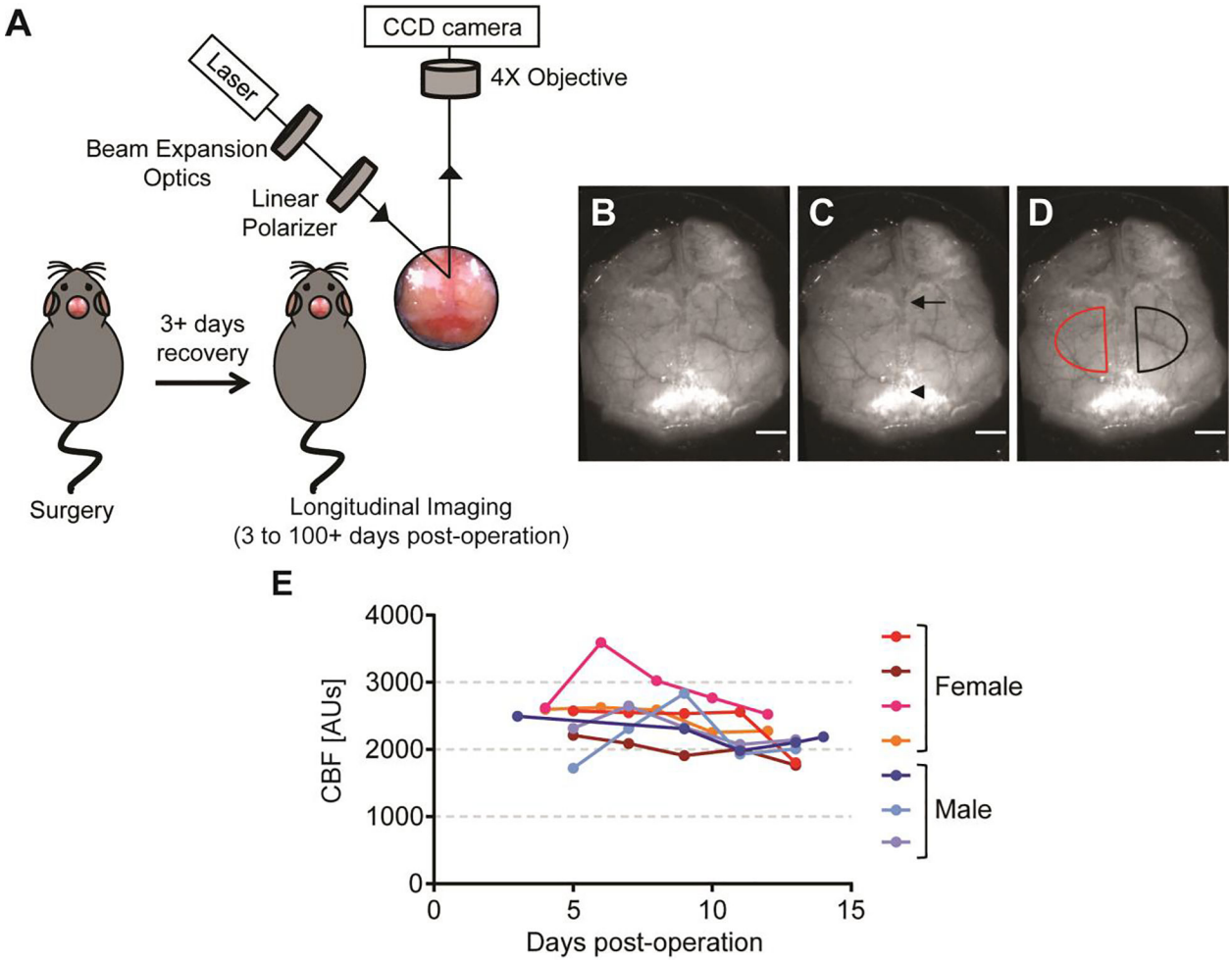

Fig. 2. Laser speckle imaging of mice.

A) Schematic of laser speckle imaging set-up. B) Example of green light image of the brain. C) Green light imaging showing bregma (arrow) and lambda (arrowhead). D) Green light image showing ROIs (half circles) over left and right side of the skull. Scale bars: 1 mm. E) Cerebral blood flow (CBF) of all animals during first two weeks.

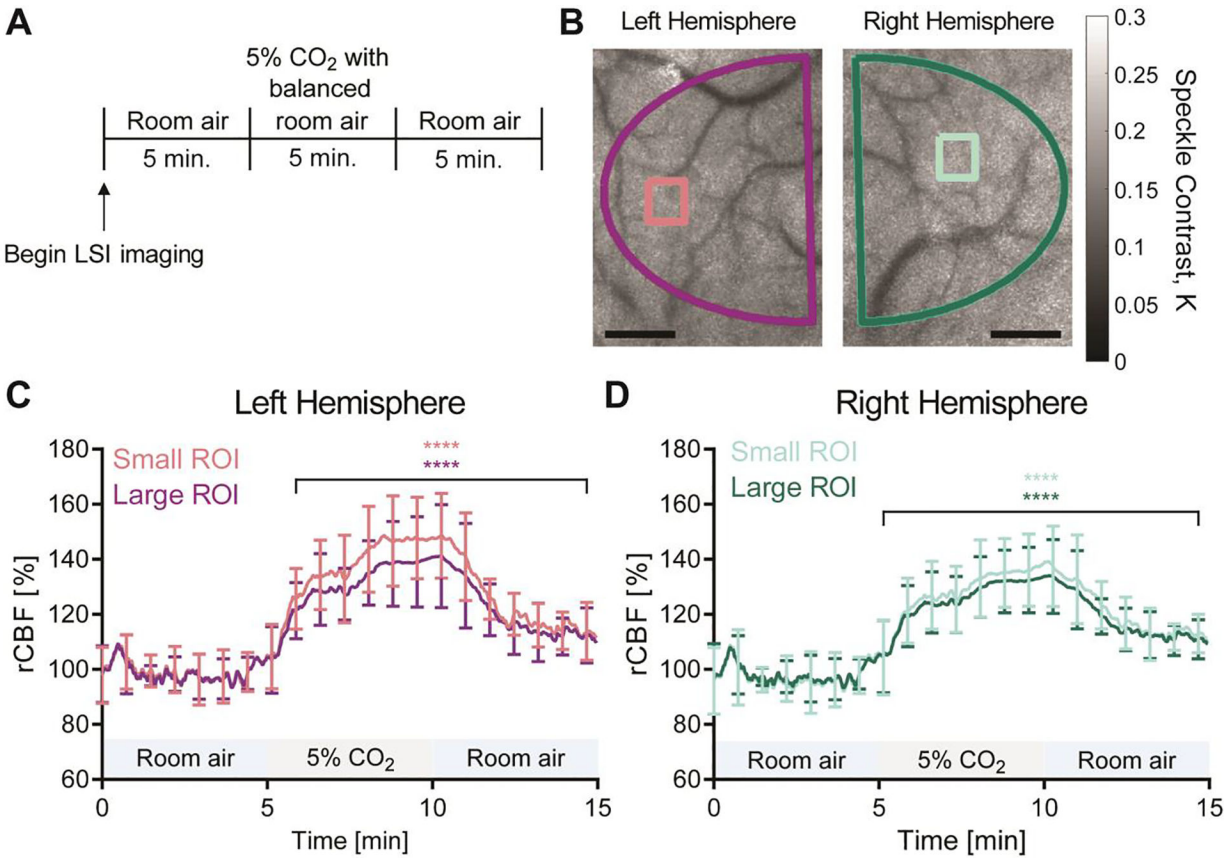

Fig. 3. Relative cerebral blood flow during hypercapnia challenge.

A) Experimental set-up of hypercapnia challenge. B) Speckle contrast image at baseline showing representative large ROIs (half circles) and small ROIs (rectangles) in the right and left hemispheres. Scale bars: 1 mm. C-D) Percent change of rCBF to baseline (prior to challenge). **** $P < 0.0001$; significance was calculated by a repeated measures two-way ANOVA, with a post-hoc Tukey test. Each time point after challenge was compared to baseline. No significant difference was found between the large and small ROIs or left and right hemisphere. Error bars represent SD.

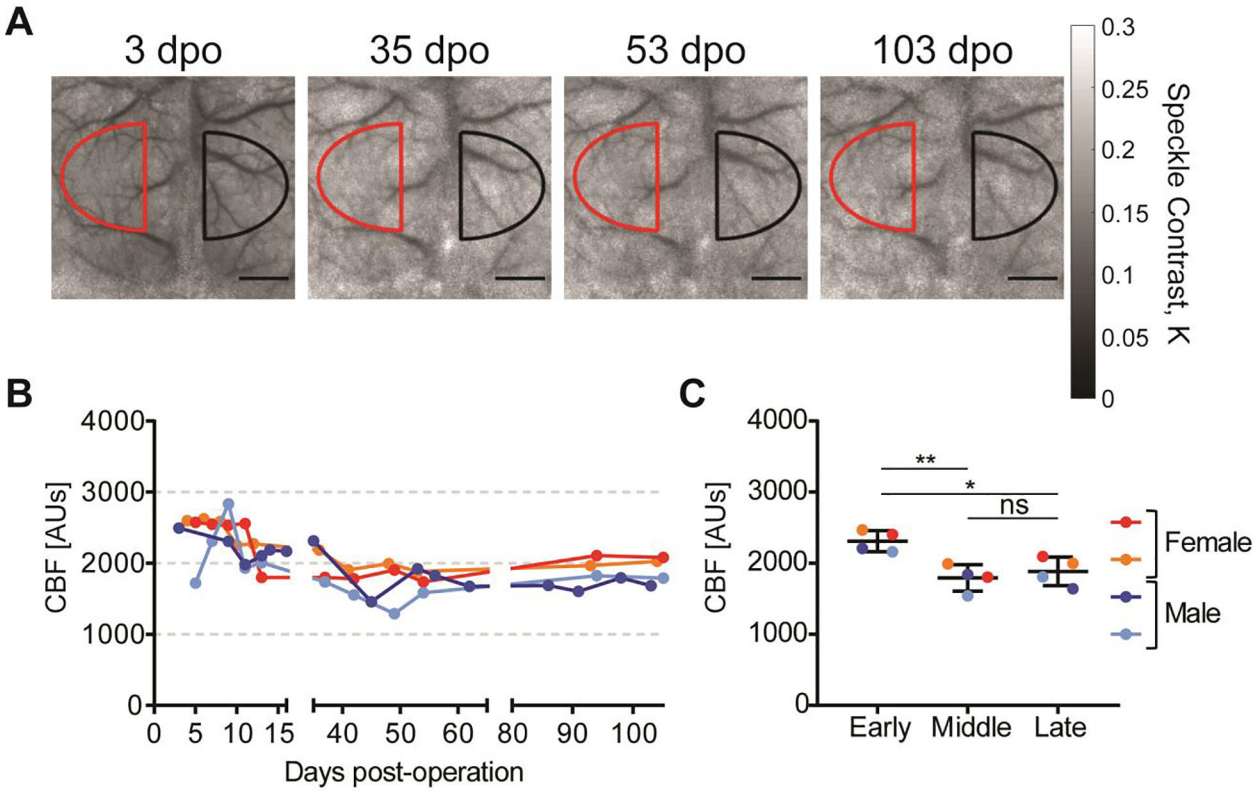

Fig. 4. Longitudinal cerebral blood flow analysis.

A) Speckle contrast imaging at 5, 35, 53, and 103 dpo. Scale bars: 1 mm. B) Longitudinal cerebral blood flow to >100 days post-operation. C) Comparison of the early (< 1 months), middle (1–2 months), and late (2+ months) time periods after surgery. * $P < 0.05$, ** $P < 0.001$, ns: not significant; significance was calculated by a repeated measures ANOVA with a Tukey post-hoc test. Error bars represent SD.